# Weld Shape Variation in Ar-$O_2$ and Ar-$CO_2$ Shielded GTA Welding†

LU Shanping *, FUJII Hidetoshi **, TANAKA Manabu ** and NOGI Kiyoshi***

**Abstract**

*The effect of the welding parameters on the GTA weld shape is systematically investigated using SUS304 stainless steel in Ar-$O_2$ and Ar-$CO_2$ mixed shielding gases. The results showed that the GTA weld shape depends to a large extent on the pattern and magnitude of the Marangoni convection on the liquid pool surface, which is controlled by the combination of the oxygen content in the weld pool and the temperature distribution on the pool surface. An outward Marangoni convection pattern will change to the inward convection mode when the oxygen content in the weld pool is over the critical value of 100ppm. Different welding parameters will change the temperature distribution and gradient on the pool surface, and therefore affect the strength of the Marangoni convection and the weld shape. A slight difference in the weld metal oxygen content from different shielding gases introduces a significantly different response in the weld depth/width ratio to the various welding parameters.*

**KEY WORDS:** (Weld Shape) (Marangoni Convection) (Oxygen) (Welding Parameter) (Stainless Steel)

## 1. Introduction

In the GTA welding of stainless steel, the weld shape is sensitive to minor elements, such as sulfur, oxygen and selenium [1-10]. Adding and precisely controlling the quantity of these minor elements in the weld pool are critical for a satisfactory weld with deep penetration [11]. Recent investigations of the effects of the oxide flux quantity [12] and active gaseous addition [11] on the weld shape variation showed that reversal of the Marangoni convection pattern was the main mechanism for changing the weld penetration which was first proposed by Heiple, Roper and Burgardt [1,2,6,10].

Since the 1980s, Debroy and co-workers have made many modeling studies to investigate the fluid flow in a weld pool for pure iron [13], carbon steel [14,15], and stainless steel [20-23] by laser spot welding or GTA spot welding. Heat transfer and fluid flow depend not only on the thermal properties of the base materials, but also on the power density and welding parameters.

In this study, the effects of Ar-$O_2$ and Ar-$CO_2$ mixed shielding gases on the weld shape were systematically investigated under variable welding parameters including welding speed, weld current and electrode gap (arc length) with a SUS304 austenitic stainless steel substrate. Based on the weld shape and weld metal oxygen content, variations of the welding parameters, the effects of oxygen in the weld pool, and pattern and magnitude of the Marangoni convection on the weld shape are discussed.

## 2. Experimental

Special SUS304 stainless plates with the average composition of 0.06%C, 0.45%Si, 0.96%Mn, 8.19%Ni, 18.22%Cr, 0.027%P, 0.0005%S, 0.0038%O and the remainder Fe, were selected for the welding experiments and machined into 100×50×10 mm rectangular plates. Four kinds of Ar-$O_2$ mixed shielding gases, Ar-0.1%$O_2$, Ar-0.3%$O_2$, Ar-0.1%$CO_2$ and Ar-0.3%$CO_2$, were selected for the welding experiments at the flow rate of 10L/Min. Partial penetration, 50mm length bead-on-plate welds were made with a Direct Current, Electrode Negative (DCEN) GTAW power supply at different welding speeds of 0.75mm/s to 5.0mm/s, welding currents of 60A to 260A and electrode gaps of 1.0mm to 9.0mm.

† Received on July 7, 2004
* Foreign Research Fellow
** Associate Professor
*** Professor

Transactions of JWRI is published by Joining and Welding Research Institute of Osaka University, Ibaraki, Osaka 567-0047, Japan

A water-cooled torch with a $\phi$2.4 mm, W-2%$ThO_2$ electrode was used. It was fixed horizontally above the positioned weld plate, which could move at different speeds using a mechanized system.

After welding, the specimens for the weld shape observations were prepared and etched by an $HCl+Cu_2SO_4$ solution to reveal the bead shape and size. The cross-sections of the weld bead were photographed using an optical microscope. The oxygen content in the weld metal was analyzed using an oxygen/nitrogen analyzer (Horiba, EMGA-520).

## 3. Results and Discussion

### 3.1 Welding current

The representative weld shapes and weld depth/width (D/W) ratio at different welding speeds under Ar-$O_2$ and Ar-$CO_2$ mixed shielding gases are shown in **Fig.1**. All the weld shapes under Ar-0.1%$O_2$ and Ar-0.1%$CO_2$ are wide and shallow, while narrow and deep weld shapes form under the Ar-0.3%$O_2$ and Ar-0.3%$CO_2$ shielding gases. The weld D/W ratio decreases with increasing welding speed for the Ar-0.3%$O_2$ and Ar-0.3%$CO_2$ shielding gases. For the Ar-0.1%$O_2$ and Ar-0.1%$CO_2$ shielding gases, the weld D/W ratio is not sensitive to the welding speed, and is about 0.2.

**Table 1** shows weld metal oxygen content at different welding speeds. The weld metal oxygen contents are around 30ppm for the Ar-0.1%$O_2$ and Ar-0.1%$CO_2$ shielding gases, and over 120ppm for the Ar-0.3%$O_2$ and Ar-0.3$CO_2$ shielding gases. When the oxygen content in the weld pool is over the critical value of around 100ppm, the Marangoni convection pattern will change from an outward direction to an inward direction during the moving GTA welding [11, 12, 22]. Therefore, an inward Marangoni convection under the Ar-0.3%$O_2$, Ar-0.3%$CO_2$ shielding gases and outward Marangoni convection under the Ar-0.1%$O_2$, Ar-0.1%$CO_2$ shielding gases occur during the welding process.

The GTA weld shape for stainless steel depends to a large extent on the direction and magnitude of the Marangoni convection, which can be expressed by the product of the temperature coefficient of the surface tension, ($d\sigma/dT$), and the temperature gradient, ($dT/dr$), on the pool surface. Changing the welding speed will alter the heat input per unit length of the weld. A high welding speed will decrease the peak temperature and the temperature gradient on the pool surface. A lower temperature gradient weakens the strength of the Marangoni convection on the pool surface, therefore, for the inward Marangoni convection mode under the Ar-0.3%$O_2$ and Ar-0.3%$CO_2$ shielding gases, the D/W ratio will decrease with the increasing welding speed as shown in **Fig.1**. However, for the outward Marangoni convection pattern under the Ar-0.1%$O_2$ and Ar-0.1%$CO_2$ shielding gases, the weak outward Marangoni convection leads to a decreasing weld width with the increasing welding speed, which will impede the decrease in the surface temperature gradient, and therefore, the weld D/W ratio is not sensitive to the increasing welding speed.

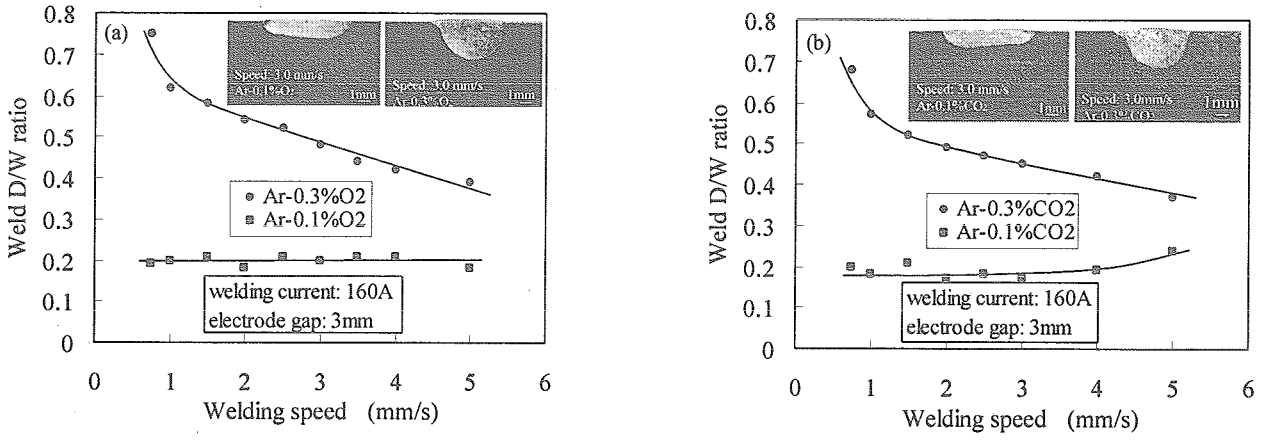


**Fig.1** Effect of welding speed on weld shape and weld D/W ratio under mixed shielding gas of (a) Ar-$O_2$ and (b) Ar-$CO_2$

**Table 1** Weld metal oxygen content at different welding speeds and shielding gases (ppm)

| Welding speed (mm/s) | 0.75 | 1.0 | 1.5 | 2.0 | 2.5 | 3.0 | 3.5 | 4.0 | 5.0 |
|---|---|---|---|---|---|---|---|---|---|
| Ar-0.1%$O_2$ | 30 | 29 | 29 | 30 | 31 | 31 | 31 | 32 | 30 |
| Ar-0.3%$O_2$ | 167 | 158 | 158 | 128 | 130 | 133 | 132 | 132 | 121 |
| Ar-0.1%$CO_2$ | 38 | 33 | 35 | 37 | 35 | 37 | --- | 43 | 47 |
| Ar-0.3%$CO_2$ | 135 | 131 | 129 | 120 | 135 | 127 | --- | 115 | 120 |

### 3.2 Welding current

The weld D/W ratio and the representative weld shapes at different welding currents under the Ar-$O_2$ and Ar-$CO_2$ mixed shielding gases are shown in **Figure 2**. The weld D/W ratio initially increases, followed by a weak decrease under the Ar-0.3%$O_2$ shielding gas or maintains a constant value of around 0.5 under the Ar-0.3%$CO_2$ shielding gas at high welding currents as shown in **Fig.2**. Under the Ar-0.1%$O_2$ and Ar-0.1%$CO_2$ shielding gases, the weld D/W ratio slightly decreases with the increasing welding current. All the weld shapes are wide and shallow under the Ar-0.1%$O_2$ and Ar-0.1%$CO_2$ shielding gases, and relatively deep and narrow weld shapes form under the Ar-0.3%$O_2$ and Ar-0.3%$CO_2$ shielding gases.

Tsai and Eagar [23] observed that increasing the welding current would increase the magnitude of the heat intensity and widen the heat distribution of the arc on the pool surface. However, the heat distribution width weakly increases compared with the magnitude of the heat density. The higher the magnitude of the heat density, the larger is the temperature gradient on the pool surface. The weld metal oxygen content is around 40ppm under the Ar-0.1%$O_2$ and Ar-0.1%$CO_2$ shielding gases as shown in **Table 2**, and an outward Marangoni convection occurs on the liquid pool in this case. The high welding current will increase the temperature gradient on the liquid pool and strengthen the outward Marangoni convection. Therefore, the weld D/W ratio weakly decreases with the increasing welding current under the Ar-0.1%$O_2$ and Ar-0.1%$CO_2$ shielding gases.

Under the Ar-0.3%$O_2$ and Ar-0.3%$CO_2$ shielding gases, the weld metal oxygen content is between 130ppm to 190ppm as shown in **Table 2**. In this case, an inward Marangoni convection occurs on the pool surface. The large welding current will increase the temperature gradient on the pool surface and strengthen the inward Marangoni convection, which will increase the weld D/W ratio as shown in Fig.2. Recently, a numerical study by Tanaka and Ushio [24. 25] showed that the convection flow in the liquid pool was mainly controlled by the plasma shear force and the Marangoni force during pure argon shielded GTA welding. A large welding current will directly increase the outward plasma shear force close to the center area of the welding pool, which will weaken the inward Marangoni convection on the pool surface. Therefore, the weld D/W ratio welding decreases or maintains a constant value around 0.5 when the welding current is over 160A under the Ar-0.3%$O_2$ and Ar-0.3%$CO_2$ shielding gases as shown in **Fig.2**.

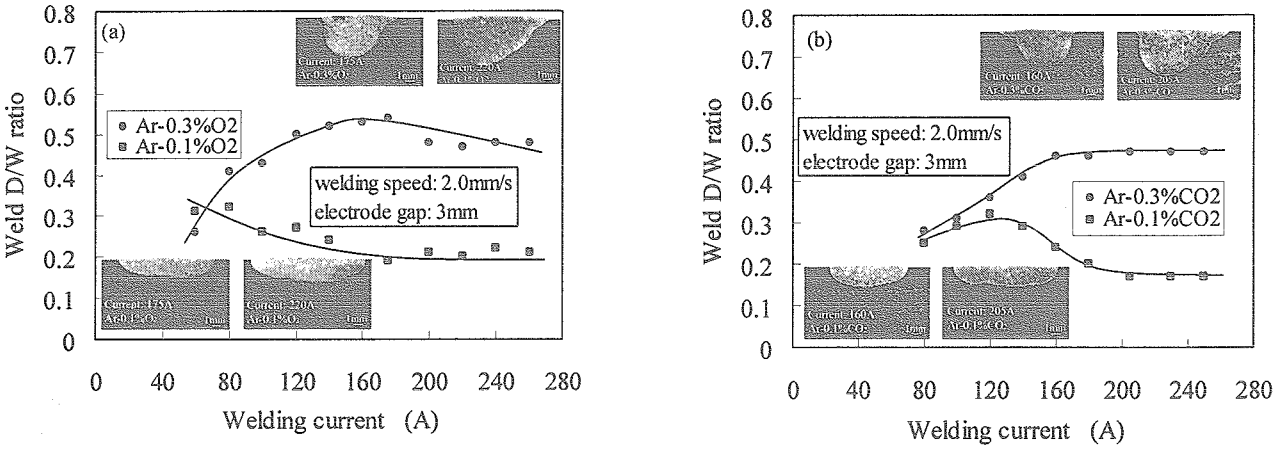


**Fig.2** Effect of welding current on weld shape and weld D/W ratio under mixed shielding gas of (a) Ar-$O_2$ and (b) Ar-$CO_2$

**Table 2** Weld metal oxygen content at different welding currents and shielding gases (ppm)

| Welding current (A) | 60 | 80 | 100 | 120 | 140 | 160 | 175 | 200 | 220 | 240 |
|---|---|---|---|---|---|---|---|---|---|---|
| Ar-0.1%$O_2$ | 56 | 50 | 34 | 34 | 34 | 29 | 31 | 51 | 48 | 49 |
| Ar-0.3%$O_2$ | 148 | 168 | 196 | 178 | 170 | 128 | 124 | 168 | 157 | 141 |
| Welding current (A) | --- | 80 | 100 | 120 | 140 | 160 | 180 | 205 | 230 | 250 |
| Ar-0.1%$CO_2$ | --- | 29 | 24 | 35 | 27 | 31 | 28 | 39 | 35 | 33 |
| Ar-0.3%$CO_2$ | --- | 175 | 194 | 197 | 181 | 168 | 160 | 147 | 135 | 134 |

### 3.3 Electrode Gap

The role of the electrode gap in determining the weld shape at a constant welding current of 160A and welding speed of 2.0mm/s for the Ar-$O_2$ and Ar-$CO_2$ shielding gases was studied by varying the arc length from 1.0 to 9.0 mm as shown in **Fig.3** and **Fig.4**. The weld D/W ratio slightly increases with the increasing electrode gap under the Ar-0.1%$O_2$ and Ar-0.1%$CO_2$ shielding gases. However, under the Ar-0.3%$O_2$ and Ar-0.3%$CO_2$ shielding gases, the weld D/W initially increases and then decreases with the increasing electrode gap as shown in **Fig.3**.

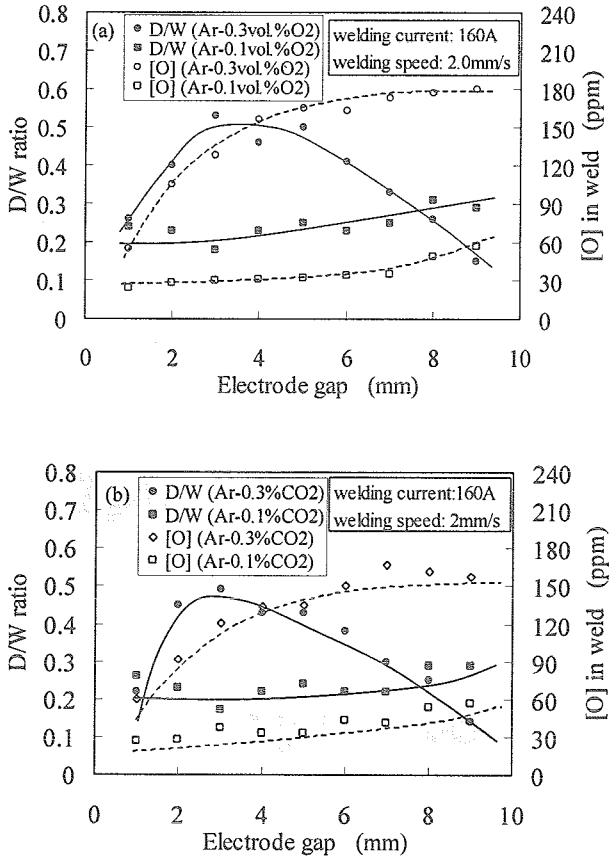


**Fig.3** Weld D/W ratio and weld metal oxygen content at different electrode gaps under mixed shielding gas of (a) Ar-$O_2$ and (b) Ar-$CO_2$

**Figure 4** shows the weld shapes for different electrode gaps under the Ar-$O_2$ mixed shielding gas. All the weld shapes are shallow and wide under the Ar-0.1%$O_2$ shielding gas. Under Ar-0.3%$O_2$ shielding gas, the weld shape for an electrode gap of 1mm is wide and shallow as shown in **Fig.4 (a)**, which is quite different from the other weld shapes shown in **Figs.4 (b, c and d)**.

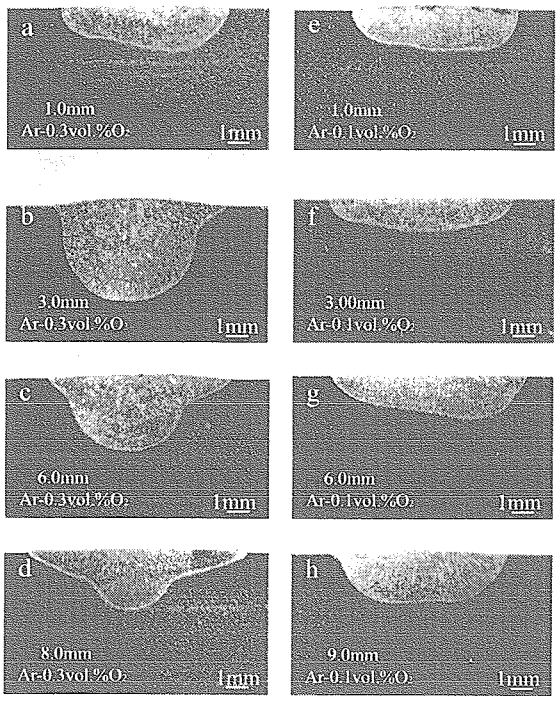


**Fig.4** Weld cross-sections at different electrode gaps under Ar-$O_2$ mixed shielding gas

At a constant welding current, the large electrode gap will directly increase the arc length and the arc voltage. Therefore, the overall heat supply from the welding power system will increase when the electrode gap increases. However, the arc efficiency will be reduced when the arc length increases [26]. Tsai reported that a large electrode gap will significantly broaden the heat distribution of the arc on the weld pool surface [23], which will enlarge the anode size and lower the heat density of the pool. Therefore, the temperature gradient on the pool surface decreases when the electrode gap increases. Ultimately, the Marangoni convection on the pool surface weakens. Based on these facts, the weld D/W ratio should decrease for the inward Marangoni convection pattern and increase for the outward Marangoni convection pattern with an increase in the electrode gap.

However, the results in **Fig. 3** shows that the weld D/W ratios under the Ar-0.3%$O_2$ and Ar-0.3%$CO_2$ shielding gases initially increase, followed by a decrease when the electrode gap is over 2mm. When the electrode gas is set at 1mm, the measured weld metal oxygen content is around 60ppm for the Ar-0.3%$O_2$ and Ar-0.3%$CO_2$ shielding gases as shown in **Fig.3**. In this case, the Marangoni convection on the liquid pool is in the outward direction. Therefore, the weld shape is wide and

shallow as shown in Fig. 4(a) and the weld D/W ratio is low.

## 4. Conclusions

Based on the results obtained, the following conclusions were reached:

(1) Oxygen is a surface active element in the stainless steel weld pool, and can be adjusted by the small additions of $O_2$ or $CO_2$ to the argon base shielding gas in GTA welding.

(2) The GTA weld shape for stainless steel depends to a large extent on the pattern and strength of the Marangoni convection on the pool surface, which is controlled by the combinations of the weld metal oxygen content and temperature distribution on the pool surface.

(3) Different welding parameters will change the weld pool temperature distribution, and therefore, affect the strength of the Marangoni convection and the weld shape. The weld D/W ratios under the Ar-0.3%$O_2$ and Ar-0.3%$CO_2$ shielding gases significantly depend on the welding parameters.

## Acknowledgements

This work is the result of "Development of Highly Efficient and Reliable Welding Technology", which is supported by the New Energy and Industrial Technology Development Organization (NEDO) through the Japan Space Utilization Promotion Center (JSUP) in the program of Ministry of Economy, Trade and Industry (METI), the 21st Century COE Program, ISIJ research promotion grant, and JFE 21st Century Foundation.

## References

1) W.S.Bennett and G.S.Mills: Welding Journal, 53 (1974), 548.
2) C.R.Heiple and J.R.Roper: Welding Journal, 60 (1981), 143.
3) Y.Takeuch, R.Takagi and T.Shinoda: Welding Journal, 71 (1992), 283.
4) M.Tanaka, T.Shimizu, H.Terasaki, M.Ushio, F.Koshi-ishi and C.L.Yang: Science and Technology of Welding and Joining, 5 (2000), 397.
5) D.S.Howse and W.Lucas: Science and Technology of Welding and Joining, 5 (2000), 189.
6) C.R.Heiple and J.R.Roper: Welding Journal, 62 (1982), 97.
7) W.Lucas and D.Howse: Weld Metal Fabrication, 64 (1996), 11.
8) T.Paskell, C.Lundin and H.Castner: Welding Journal, 76 (1997), 57.
9) Y.Wang and H.L.Tsai: Metallurgical and Materials Transactions B, 32 (2001), 501.
10) C.R.Heiple and P.Burgardt: Welding Journal, 64 (1985), 159.
11) S.P.Lu, H.Fujii, H.Sugiyama, M.Tanaka and K.Nogi: ISIJ Int., 43 (2003), 1590.
12) S.P.Lu, H.Fujii, H.Sugiyama, M.Tanaka and K.Nogi: Mater. Trans., 43 (2002), 2926.
13) A.Paul and T.Debroy: Metall. Trans. B: 19 (1988), 851.
14) W.Pitscheneder, T.Debroy, K.Mundra and R.Ebner: Welding Journal, 75 (1996), 71.
15) W.Zhang, G.G.Roy, J.W.Elmer and T.Debroy: J. Appl. Phys., 93 (2003), 3022.
16) T.Zacharia, S.A.David, J.M.Vitek and T.Debroy: Welding Journal, 68 (1989), 499.
17) T.Zacharia, S.A.David, J.M.Vitek and T.Debroy: Welding Journal, 68 (1989), 510.
18) X.He, P.W.Fuerschbach and T.Debroy: J. Phys. D: Appl. Phys., 36 (2003), 1388.
19) K.Mundra and T.Debroy: Metall. Trans. B, 24 (1993), 145.
20) T.Zacharia, S.A.David, M.M.Vitek and T.Debroy: Metall. Trans. B, 21 (1990), 600.
21) Y.Wang and H.L.Tsai: Int. J Heat Mass Trans., 44 (2001), 2067.
22) S.P.Lu, H.Fujii and K.Nogi: Metallurgical and Materials Transactions A, (2004), (accepted).
23) N.S.Tsai and T.W.Eagar: Metall. Trans.B, 16 (1985), 841.
24) M.Tanaka, H.Terasaki, M.Ushio and J.J.Lowke: Plasam Chem. Plasma Process., 23 (2003), 585.
25) M.Ushio, M.Tanaka and J.J.Lowke: IEEE Trans. On Plasma Sci., 32 (2004), 108.
26) P.Burgardt and C.R.Heiple: Welding Journal, 65 (1986), 150.